THE JOURNAL OF PHYSICAL CHEMISTRY Letters

Letter

Cite This: J. Phys. Chem. Lett. 2018, 9, 3131−3136

pubs.acs.org/JPCL

Water Dissociates at the Aqueous Interface with Reduced Anatase TiO_2 (101)

Immad M. Nadeem,[†,‡] Jon P. W. Treacy,[§] Sencer Selcuk,[∥] Xavier Torrelles,[⊥] Hadeel Hussain,[§] Axel Wilson,[†] David C. Grinter,[†] Gregory Cabailh,[#] Oier Bikondoa,[▽,○] Christopher Nicklin,[‡] Annabella Selloni,[∥] Jörg Zegenhagen,[‡] Robert Lindsay,[§] and Geoff Thornton*[,†]

[†]London Centre for Nanotechnology and Department of Chemistry, University College London, 20 Gordon Street, London, WC1H 0AJ, United Kingdom

[‡]Diamond Light Source Ltd, Harwell Science and Innovation Campus, Didcot, Oxfordshire OX11 0DE, United Kingdom

[§]Corrosion and Protection Centre, School of Materials, The University of Manchester, Sackville Street, Manchester M13 9PL, United Kingdom

[∥]Department of Chemistry, Princeton University, Princeton, New Jersey 08540, United States

[⊥]Institut de Ciència de Materials de Barcelona (CSIC), Campus UAB, 08193 Bellaterra, Spain

[#]Sorbonne Université, CNRS, UMR 7588, Institut des NanoSciences de Paris, 4 Place Jussieu, F-75005 Paris, France

[▽]Department of Physics, University of Warwick, Gibbet Hill Road, Coventry CV4 7AL, United Kingdom

[○]XMaS, the U.K. CRG Beamline, ESRF, The European Synchrotron, 71, Avenue des Martyrs, CS40220, F-38043 Grenoble Cedex 09, France

Supporting Information

ABSTRACT: Elucidating the structure of the interface between natural (reduced) anatase TiO_2 (101) and water is an essential step toward understanding the associated photoassisted water splitting mechanism. Here we present surface X-ray diffraction results for the room temperature interface with ultrathin and bulk water, which we explain by reference to density functional theory calculations. We find that both interfaces contain a 25:75 mixture of molecular H_2O and terminal OH bound to titanium atoms along with bridging OH species in the contact layer. This is in complete contrast to the inert character of room temperature anatase TiO_2 (101) in ultrahigh vacuum. A key difference between the ultrathin and bulk water interfaces is that in the latter water in the second layer is also ordered. These molecules are hydrogen bonded to the contact layer, modifying the bond angles.

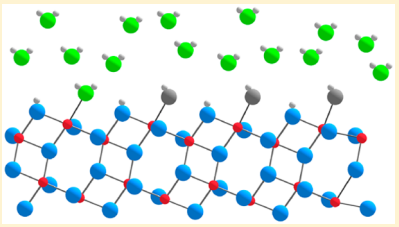

Ever since Honda and Fujishima[1] demonstrated photoassisted water splitting on titanium dioxide (TiO_2), it has been widely investigated for hydrogen fuel production.[2] Determining the interface structures of well-defined TiO_2 surfaces and water is a crucial step toward understanding this process on an atomic scale. Rutile TiO_2 (110) (R_{110}) and anatase TiO_2 (101) (A_{101}) have been the focus of numerous surface science studies. While the structure of the R_{110}/H_2O interface has been studied in a number of environments,[3,4] studies of A_{101} have so far been largely restricted to ultrahigh vacuum (UHV).[5−13] A surface science perspective of water on brookite[14] is limited to simulations.

The A_{101} surface consists of 5-fold (Ti_{5c}) and 6-fold (Ti_{6c}) coordinated Ti atoms and 2-fold (O_{2c}) and 3-fold (O_{3c}) coordinated O atoms in a sawtooth geometry (see Figure 1).[15,16] Water does not adsorb on A_{101} in UHV conditions at room temperature, although it adsorbs molecularly on Ti_{5c} at low temperature.[5] Dissociative adsorption to form terminal OH (OH_t)[6,7] (i.e., OH adsorbed to Ti_{5c}) and/or bridging OH (OH_{br})[12,13] has been reported following electron[12,13] and photon excitation[9] as well as coadsorption with O_2[6,7] at low temperature. There is evidence from photoemission spectros-

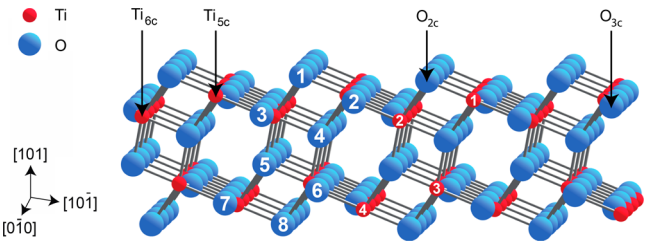

Figure 1. Ball and stick model of A_{101} (1 × 1). The numerical labeling of the atoms serves as identification for the atomic displacements shown in Table 1. The indicated azimuth defines the *x*, *y*, and *z* directions along which the atomic coordinates are defined as positive.

Received: April 16, 2018
Accepted: May 16, 2018
Published: May 16, 2018

DOI: 10.1021/acs.jpclett.8b01182
J. Phys. Chem. Lett. 2018, 9, 3131−3136

Table 1. Experimental (SXRD) and Theoretical (DFT) Surface Atomic Displacements Away from the Bulk Terminated Structure of A_{101}[a]

	displacements (Å)					
	A_{101}/UHV (as-prepared)		A_{101}/ultrathin water film		A_{101}/bulk water	
atom label	Δ [10$\bar{1}$] [16SXRD[b]:SXRD[c]:DFT]	Δ [101] [16SXRD[b]:SXRD[c]:DFT]	Δ [10$\bar{1}$] [SXRD:DFT]	Δ [101] [SXRD:DFT]	Δ [10$\bar{1}$] [SXRD:DFT]	Δ [101] [SXRD:DFT]
O-1	0.11:0.14:0.23	0.07:0.10:0.02	0.05:−0.01	−0.01:0.08	−0.03:−0.05	0.03:0.05
Ti-1	0.03:0.02:−0.01	0.01: −0.01:−0.12	0.02:0.00	0.07:0.15	−0.02:−0.06	0.11:0.13
O-2	0.11:0.13:0.14	0.15:0.14:0.25	−0.08:−0.02	0.12:0.16	−0.03:−0.04	0.09:0.17
O-3	0.18:0.16:0.11	0.08:0.05:0.06	−0.08:−0.04	0.10:0.00	−0.04:−0.09	0.04:0.01
Ti-2	0.12:0.11:0.12	0.15:0.16:0.21	0.08:−0.03	0.09:0.01	0.02:−0.07	0.06:0.03
O-4	−0.01:0.01:0.13	0.01:0.01:−0.02	0.15:−0.04	0.00:0.07	0.04:−0.05	0.01:0.08
O-5	−0.07:−0.04:0.05	0.06:0.06:0.06	−0.03:−0.03	−0.03:0.04	0.05:−0.04	0.04:0.04
Ti-3	0.01:−0.01:−0.05	0.04:0.03:−0.05	0.06:−0.02	0.06:0.07	0.05:−0.03	0.05:0.07
O-6	−0.06:−0.05:−0.01	0.05:0.07:0.02	−0.13:−0.03	0.07:0.06	−0.04:−0.03	0.05:0.07
O-7	0.13:0.14:0.01	0.08:0.05:0.04	0.01:−0.03	0.04:0.05	0.05:−0.04	0.02:0.05
Ti-4	0.06:0.08:0.01	0.08:0.09:0.10	0.07:−0.03	0.07:0.03	0.03:−0.04	0.03:0.04
O-8	−0.05:−0.04:−0.01	0.00:0.04:0.02	0.03:−0.03	0.00:0.04	0.01:−0.03	0.01:0.05

[a]Positive or negative displacements indicate those parallel or anti-parallel to the directions of the coordinate axis defined in Figure 1. Experimental errors correspond to ±0.01 Å as obtained from the fitting procedure. [b]Represents as-prepared surface before formation of the ultrathin water film interface (10 ± 2 layers). [c]Represents as-prepared surface before formation of the bulk water interface.

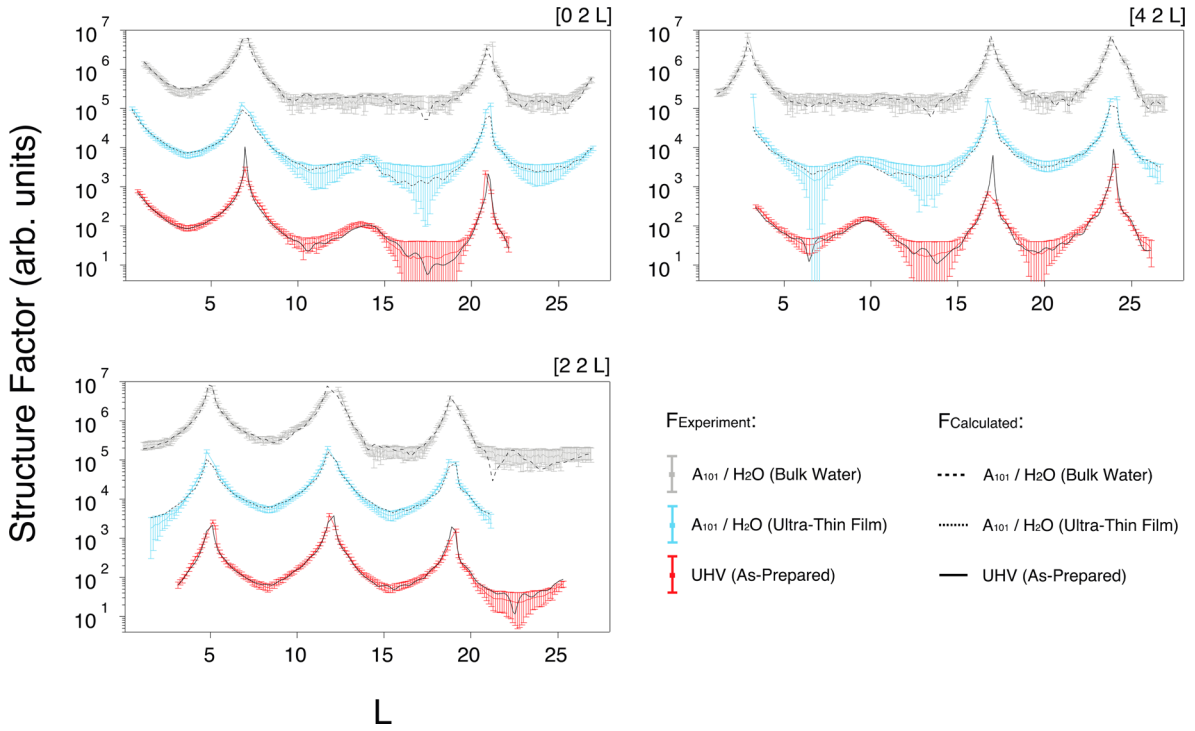

Figure 2. Comparison of experimental CTRs for as-prepared A_{101} in UHV[16] (red), and for the A_{101} interface with an ultrathin water film (blue) and bulk water (gray). CTRs are offset for clarity. A full set of CTRs and their respective best fit is given in the SI (see Figures S1 and S2). $F_{Experiment}$: experimental structure factor. $F_{Calculated}$: calculated structure factor.

copy of mixed molecular-dissociative adsorption at room temperature at a higher pressure of water (0.6−6.0 mbar).[17]

The reduced room temperature reactivity of A_{101} to water in UHV compared with R_{110} is thought to be due to the lack of surface oxygen vacancies.[18] These vacancies, which promote dissociation on R_{110},[19] are absent on A_{101} because they are more stable in subsurface sites.[18] However, the unreactive character of reduced A_{101} in UHV is predicted to be modified when a liquid interface is formed by trapping excess electrons at bound hydroxyl complexes.[10] Here we test this idea through a quantitative structure determination of the A_{101} surface covered by an ultrathin water film or bulk water, complemented with density functional theory (DFT) calculations. We find that a mixture of molecular and dissociated water is present in the contact layer, pointing to a significantly enhanced reactivity of the substrate compared with that observed in UHV.

The interface structures for A_{101} with an ultrathin film and bulk water were obtained from surface X-ray diffraction (SXRD) data in comparison with DFT calculations. SXRD data recorded from the clean surface in UHV prior to the interface measurements are essentially identical to those published previously.[16] Labeling of titanium and oxygen

DOI: 10.1021/acs.jpclett.8b01182
J. Phys. Chem. Lett. 2018, 9, 3131−3136

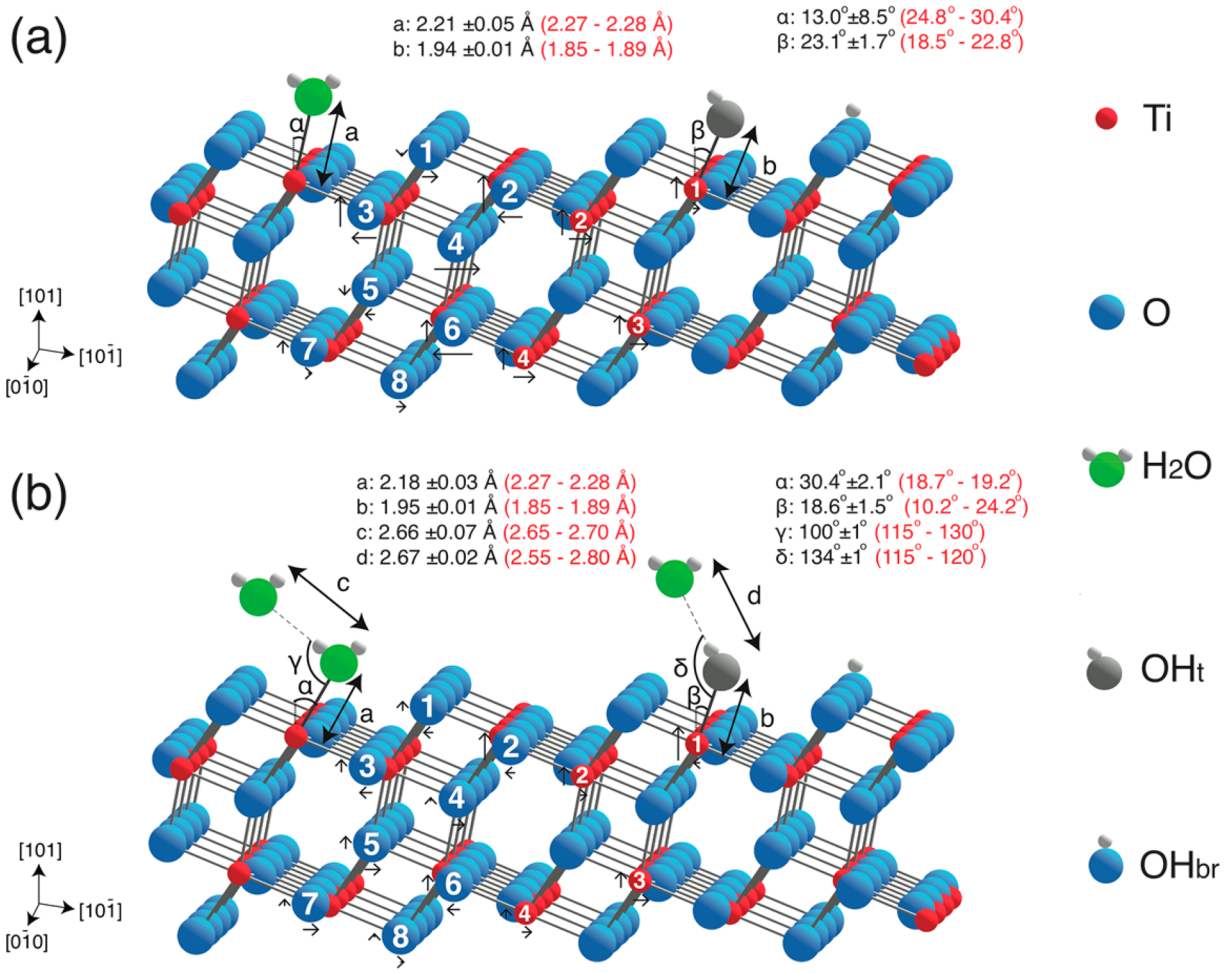

Figure 3. Ball and stick model of the proposed A_{101} interface with (a) an ultrathin water film and (b) bulk water. Experimental (SXRD) bond lengths and angles are presented in black, with DFT calculations denoted in red. The black arrows represent the relative magnitude and direction of atom displacements with respect to bulk lattice positions. Hydrogen atoms were not included in the experimental fitting procedure due to their small X-ray scattering strength, and so are only displayed for illustrative purposes. A complete coverage of adsorbed H_2O/OH on Ti_{5c} is proposed. However, for presentation purposes, this figure shows only one adsorbed H_2O and OH_t.

atoms used here is identical to that used in our previous work[16] (see Figure 1). The atomic displacements on the as-prepared surface, given in Table 1, indicate a relaxation of atoms away from the bulk, a phenomenon previously observed on R_{110} in UHV.[20] As discussed in our previous work,[16] surface roughness has been modeled with a "terraced roughness"[21] approach, which allows better simulation of the step-related surface roughness. Modeling is performed with two surface domains with identical terminations that differ in the relative height from the bulk at which the termination occurs. Occupancy of the two domains is in a 1:3 ratio as in our previous work.[16]

Three experimental crystal truncations rods (CTRs) and the best fits for A_{101} covered with a 10 ± 2 monolayer water film (see SI for details) and bulk water are shown in Figure 2, with the complete data sets in Figures S1 and S2, respectively. The A_{101} surface atomic displacements before and after formation of the water interface are shown in Table 1. These optimized atomic displacements indicate mixed associative and dissociative water adsorption with a normalized χ^2 (χ^2_n) of 1.12 and 1.05 for the ultrathin water film and bulk water, respectively. The nonuniform agreement between certain experimental and DFT displacements is largely attributed to calculation limitations. Displacements were determined by considering the difference of the optimized atomic positions without sampling different atomic configurations, as would be more appropriate at finite temperature, especially at the aqueous interface.

The best-fit SXRD model for the A_{101} interface with the ultrathin water film suggests ordering in the contact layer only, with a complete coverage of adsorbed H_2O/OH species on Ti_{5c} (Ti-1). There are two distinct Ti_{5c}–OH_2/OH species with 25% and 75% coverage and bond lengths of 2.21 ± 0.04 Å and 1.94 ± 0.01 Å, respectively (see Figure 3 and see Figure S3a for a graph of χ^2_n against a change in surface adsorbate coverage). The best-fit SXRD model for the interface with bulk water has an additional ordered layer above the contact layer. Similar to the ultrathin case, the contact layer contains two distinct Ti_{5c}–OH_2/OH species with 25% and 75% surface coverage and bond lengths of 2.18 ± 0.03 Å and 1.95 ± 0.01 Å, respectively (see Figure 3 and see Figure S3a for a graph of χ^2_n against a change in surface adsorbate coverage). The second layer appears to consist of H_2O molecules that are hydrogen bonded to molecules in the contact layer based on the bond distances (see Figure 3). Interestingly, as is shown in Figure 3, the bond angle of the H_2O and OH_t species on Ti_{5c} (Ti-1) varies depending on whether the surface is contacted with the

DOI: 10.1021/acs.jpclett.8b01182
J. Phys. Chem. Lett. 2018, 9, 3131−3136

ultrathin film or bulk water. This can be attributed to the presence of the ordered second layer in the case of the bulk water interface (see Figure S3b for a graph of χ^2_n against a change in second monolayer coverage).

Previous DFT and molecular dynamics (MD) simulations[22−31] predict a $Ti_{5c}-O_{H_2O}$ bond length in the range 2.15−2.30 Å, while the $Ti_{5c}-O_{OH}$ bond length is predicted to be 1.80−1.90 Å. Our current DFT calculations predict the $Ti_{5c}-OH_2$ bond length to be 2.27−2.28 Å and the $Ti_{5c}-OH_t$ bond length to be 1.85−1.89 Å (see Figure 3). Experimental measurements of the $R_{110}/H_2O_{(l)}$ interface show a $Ti_{5c}-OH_t$ bond length at 1.95 ± 0.03 Å.[4] On this basis, the Ti_{5c}-O bond lengths of 2.21 ± 0.05 Å (ultrathin film) and 2.18 ± 0.03 Å (bulk water) can be attributed to associative H_2O surface adsorption on Ti_{5c}, while the bond lengths of 1.94 ± 0.01 Å (ultrathin film) and 1.95 ± 0.01 Å (bulk water) correspond to dissociative adsorption to form $Ti_{5c}-OH_t$. A 25% occupation of Ti_{5c} sites by molecular water was also found in UHV scanning tunneling microscopy (STM) images following exposure of A_{101} to water vapor at 6 K.[5] At low temperature this forms a locally ordered 2 × 2 overlayer, which could in principle be present at the ultrathin water film and bulk water interface. The small domain size would prevent fractional order rods (FORs) from being observed.

The surface atomic displacements after formation of the aqueous interfaces are in general close to zero. In other words, the expansion of the surface observed in UHV is reversed with the formation of the interface. This behavior has been previously observed at the R_{110}/H_2O interface[4] and is well reproduced by our DFT calculations. Interestingly, experiment and theory suggest an expansion away from the bulk for the Ti_{5c} (Ti-1) atom. This movement is attributed to the formation of Ti_{5c} (Ti-1) bonds to OH_2/OH in the contact layer. The experimental bond angles associated with molecules in the contact layer (see Figure 3) are reproduced reasonably well by our theoretical calculations. Any discrepancies can be attributed to limitations associated with the optb88-vdw DFT functional. This functional has been shown to simulate the aqueous environment better than the Perdew, Burke, and Ernzerhof (PBE) functional[32,33] and has been used to describe several semiconductor/water interfaces accurately, although its suitability to reproduce bond angles is as yet unclear.[32−35]

Previous calculations of the A_{101}/water interface predict that the formation of OH_t species from water dissociation is coupled with the formation of OH_{br} species that trap excess electrons from the selvedge.[10] In principle, this can be probed experimentally by the position of the O_{2c} to which a H atom is bound to form OH_{br}.[27] Our SXRD results indicate that, after H_2O exposure, the $Ti_{5c}-O_{2c}$ bond length increases from 1.90 ± 0.02 Å to 1.95 ± 0.01 Å and 1.88 ± 0.01 Å to 1.95 ± 0.01 Å, respectively for the ultrathin water film and bulk water interfaces. Earlier calculations[27] predict that the $Ti_{5c}-O_{2c}$ bond length is 1.86 Å for the clean surface, which can increase up to 1.88 Å in the presence of OH_t and H_2O species at the Ti_{5c} (Ti-1) site. However, in the presence of both OH_{br} and OH_t species, the $Ti_{5c}-O_{2c}$ bond length can increase up to 2.01 Å. This is supported by our current DFT calculations, which show that the presence of OH_{br} species can result in a Ti_{5c}-O_{2c} bond length of ∼2 Å, whereas in the absence of OH_{br} and with only H_2O or OH_t adsorption at the Ti_{5c} site, the Ti_{5c}-O_{2c} bond length is ∼1.85 Å. Given that our experimental findings indicate an expansion of the Ti_{5c}-O_{2c} bond length after aqueous interface formation, it can be inferred that the interface consists of OH_{br} species formed via H_2O dissociation to form OH_t and OH_{br} species.

The influence of the water layer thickness on the contact layer structure has been discussed in the literature, although there has been a lack of experimental evidence.[36] In our work, we observe that our ultrathin water film and bulk water on A_{101} induces a similar contact layer with differences arising from an ordered second monolayer at the A_{101}/bulk water interface. This indicates that the ultrathin water film thickness of 10 ± 2 monolayers[37] is below that required for it to behave as bulk water. The activation of A_{101} to induce water dissociation at the aqueous interface while being inert in UHV can be explained in terms of the interplay between excess electrons and adsorbed water. Although little electron trapping is observed at the surface of as-prepared A_{101} in UHV, an excess electron at the aqueous interface can trigger water dissociation to form surface OH species.[10] The catalytic activation of A_{101} under aqueous conditions can be explained by the interaction of excess electrons with multiple water layers and the subsequent electron trapping at the resultant OH species.

In conclusion, this study has shown that room temperature aqueous interfaces with reduced A_{101} have a mixture of molecular H_2O (25%) and OH_t (75%) bound to Ti_{5c} in the contact layer. OH_t formation from water dissociation is accompanied by the formation of OH_{br}. On the basis of previous calculations,[10] the reduced state of the anatase will play a crucial role in the formation of this contact layer since it provides the excess electrons needed for dissociation. Upon water exposure to the as-prepared surface, the surface atoms contract toward the bulk and adopt a relatively more bulk-like appearance when compared to the as-prepared surface. This study highlights the importance of the substrate environment in determining its reactivity. For A_{101}, the aqueous interface is reactive, whereas the UHV substrate is inert at room temperature. Since the aqueous interface is relevant in photocatalysis, it also highlights the importance of studies in realistic environments. This behavior of A_{101} is likely to be observed on other reducible metal oxides; however, this will depend on its surface electronic structure. For instance, in contrast to the (101) termination, the (001) termination of anatase does not trap electrons.[10]

■ ASSOCIATED CONTENT

Supporting Information

The Supporting Information is available free of charge on the ACS Publications website at DOI: 10.1021/acs.jpclett.8b01182.

Experimental and computational methods, CTRs with the best fit for the A_{101} interface with an ultrathin water film and the A_{101} interface with bulk water, and a χ^2_n graph highlighting the change in χ^2_n against a change in surface adsorbate coverage (PDF)

■ AUTHOR INFORMATION

Corresponding Author

*E-mail: g.thornton@ucl.ac.uk.

ORCID

Xavier Torrelles: 0000-0002-6891-7793
Annabella Selloni: 0000-0001-5896-3158
Geoff Thornton: 0000-0002-1616-5606

DOI: 10.1021/acs.jpclett.8b01182
J. Phys. Chem. Lett. 2018, 9, 3131−3136

Notes

The authors declare no competing financial interest.

■ ACKNOWLEDGMENTS

This work was supported by the European Research Council Advanced Grant ENERGYSURF to GT, EPSRC (EP/L015862/1), EU COST Action CM1104, EU Fund for Regional Development POCTFA through Project EFA194/16/TNSI, and the Royal Society (UK) through a Wolfson Research Merit Award and M.E.C. (Spain) through Project MAT2015-68760-C2-2-P. A.S and S.S thank DoE-BES, Division of Chemical Sciences, Geosciences, and Biosciences support under Award No. DE-SC0007347 and NERSC (DoE) Contract No. DE-AC02-05CH11231. This work was carried out with the support of Diamond Light Source - Proposals SI8634 and SI11345.

■ REFERENCES

(1) Fujishima, A.; Honda, K. Electrochemical Photolysis of Water at a Semiconductor Electrode. *Nature* **1972**, *238*, 37−38.
(2) Chen, X. B.; Shen, S. H.; Guo, L. J.; Mao, S. S. Semiconductor-Based Photocatalytic Hydrogen Generation. *Chem. Rev.* **2010**, *110*, 6503−6570.
(3) Pang, C. L.; Lindsay, R.; Thornton, G. Chemical Reactions on Rutile TiO_2 (110). *Chem. Soc. Rev.* **2008**, *37*, 2328−2353.
(4) Hussain, H.; Tocci, G.; Woolcot, T.; Torrelles, X.; Pang, C. L.; Humphrey, D. S.; Yim, C. M.; Grinter, D. C.; Cabailh, G.; Bikondoa, O.; et al. Structure of a Model TiO_2 Photocatalytic Interface. *Nat. Mater.* **2017**, *16*, 461−466.
(5) He, Y. B.; Tilocca, A.; Dulub, O.; Selloni, A.; Diebold, U. Local Ordering and Electronic Signatures of Submonolayer Water on Anatase TiO_2 (101). *Nat. Mater.* **2009**, *8*, 585−589.
(6) Setvin, M.; Daniel, B.; Aschauer, U.; Hou, W.; Li, Y. F.; Schmid, M.; Selloni, A.; Diebold, U. Identification of Adsorbed Molecules via STM Tip Manipulation: CO, H_2O, and O_2 on TiO_2 Anatase (101). *Phys. Chem. Chem. Phys.* **2014**, *16*, 21524−21530.
(7) Setvin, M.; Aschauer, U.; Hulva, J.; Simschitz, T.; Daniel, B.; Schmid, M.; Selloni, A.; Diebold, U. Following the Reduction of Oxygen on TiO_2 Anatase (101) Step by Step. *J. Am. Chem. Soc.* **2016**, *138*, 9565−9571.
(8) Walle, L. E.; Borg, A.; Johansson, E. M. J.; Plogmaker, S.; Rensmo, H.; Uvdal, P.; Sandell, A. Mixed Dissociative and Molecular Water Adsorption on Anatase TiO_2 (101). *J. Phys. Chem. C* **2011**, *115*, 9545−9550.
(9) Geng, Z. H.; Chen, X.; Yang, W. S.; Guo, Q.; Xu, C. B.; Dai, D. X.; Yang, X. M. Highly Efficient Water Dissociation on Anatase TiO_2 (101). *J. Phys. Chem. C* **2016**, *120*, 26807−26813.
(10) Selcuk, S.; Selloni, A. Facet-Dependent Trapping and Dynamics of Excess Electrons at Anatase TiO_2 Surfaces and Aqueous Interfaces. *Nat. Mater.* **2016**, *15*, 1107−1113.
(11) Futera, Z.; English, N. J. Exploring Rutile (110) and Anatase (101) TiO_2 Water Interfaces by Reactive Force-Field Simulations. *J. Phys. Chem. C* **2017**, *121*, 6701−6711.
(12) Nadeem, I. M.; Harrison, G. T.; Wilson, A.; Pang, C. L.; Zegenhagen, J.; Thornton, G. Bridging Hydroxyls on Anatase TiO_2 (101) by Water Dissociation in Oxygen Vacancies. *J. Phys. Chem. B* **2018**, *122*, 834−839.
(13) Payne, D. T.; Zhang, Y.; Pang, C. L.; Fielding, H. H.; Thornton, G. Creating Excess Electrons at the Anatase TiO_2 (101) Surface. *Top. Catal.* **2017**, *60*, 392−400.
(14) Holmstrom, E.; Ghan, S.; Asakawa, H.; Fujita, Y.; Fukuma, T.; Kamimura, S.; Ohno, T.; Foster, A. S. Hydration Structure of Brookite TiO_2 (210). *J. Phys. Chem. C* **2017**, *121*, 20790−20801.
(15) Hebenstreit, W.; Ruzycki, N.; Herman, G. S.; Gao, Y.; Diebold, U. Scanning Tunneling Microscopy Investigation of the TiO_2 Anatase (101) Surface. *Phys. Rev. B: Condens. Matter Mater. Phys.* **2000**, *62*, R16334−R16336.
(16) Treacy, J. P. W.; Hussain, H.; Torrelles, X.; Grinter, D. C.; Cabailh, G.; Bikondoa, O.; Nicklin, C.; Selcuk, S.; Selloni, A.; Lindsay, R.; et al. Geometric Structure of Anatase TiO_2 (101). *Phys. Rev. B: Condens. Matter Mater. Phys.* **2017**, *95*, 075416.
(17) Jackman, M. J.; Thomas, A. G.; Muryn, C. Photoelectron Spectroscopy Study of Stoichiometric and Reduced Anatase TiO_2 (101) Surfaces: The Effect of Subsurface Defects on Water Adsorption at Near-Ambient Pressures. *J. Phys. Chem. C* **2015**, *119*, 13682−13690.
(18) Scheiber, P.; Fidler, M.; Dulub, O.; Schmid, M.; Diebold, U.; Hou, W. Y.; Aschauer, U.; Selloni, A. (Sub)Surface Mobility of Oxygen Vacancies at the TiO_2 Anatase (101) Surface. *Phys. Rev. Lett.* **2012**, *109*, 136103.
(19) Bikondoa, O.; Pang, C. L.; Ithnin, R.; Muryn, C. A.; Onishi, H.; Thornton, G. Direct Visualization of Defect-Mediated Dissociation of Water on TiO_2 (110). *Nat. Mater.* **2006**, *5*, 189−192.
(20) Cabailh, G.; Torrelles, X.; Lindsay, R.; Bikondoa, O.; Joumard, I.; Zegenhagen, J.; Thornton, G. Geometric Structure of TiO_2 (110) (1 × 1): Achieving Experimental Consensus. *Phys. Rev. B: Condens. Matter Mater. Phys.* **2007**, *75*, 241403.
(21) Magdans, U.; Gies, H.; Torrelles, X.; Rius, J. Investigation of the {104} Surface of Calcite under Dry and Humid Atmospheric Conditions with Grazing Incidence X-ray Diffraction (GIXRD). *Eur. J. Mineral.* **2006**, *18*, 83−91.
(22) Tilocca, A.; Selloni, A. Structure and Reactivity of Water Layers on Defect-Free and Defective Anatase TiO_2 (101) Surfaces. *J. Phys. Chem. B* **2004**, *108*, 4743−4751.
(23) Aschauer, U. J.; Tilocca, A.; Selloni, A. Ab Initio Simulations of the Structure of Thin Water Layers on Defective Anatase TiO_2 (101) Surfaces. *Int. J. Quantum Chem.* **2015**, *115*, 1250−1257.
(24) Patrick, C. E.; Giustino, F. Structure of a Water Monolayer on the Anatase TiO_2 (101) Surface. *Phys. Rev. Appl.* **2014**, *2*, 014001.
(25) Zhao, Z. Y.; Li, Z. S.; Zou, Z. G. A Theoretical Study of Water Adsorption and Decomposition on the Low-Index Stoichiometric Anatase TiO_2 Surfaces. *J. Phys. Chem. C* **2012**, *116*, 7430−7441.
(26) Aschauer, U.; He, Y. B.; Cheng, H. Z.; Li, S. C.; Diebold, U.; Selloni, A. Influence of Subsurface Defects on the Surface Reactivity of TiO_2: Water on Anatase (101). *J. Phys. Chem. C* **2010**, *114*, 1278−1284.
(27) Vittadini, A.; Selloni, A.; Rotzinger, F. P.; Gratzel, M. Structure and Energetics of Water Adsorbed at TiO_2 Anatase (101) and (001) Surfaces. *Phys. Rev. Lett.* **1998**, *81*, 2954−2957.
(28) Sumita, M.; Hu, C. P.; Tateyama, Y. Interface Water on TiO_2 Anatase (101) and (001) Surfaces: First-Principles Study with TiO_2 Slabs Dipped in Bulk Water. *J. Phys. Chem. C* **2010**, *114*, 18529−18537.
(29) Gong, X. Q.; Selloni, A.; Batzill, M.; Diebold, U. Steps on Anatase TiO_2 (101). *Nat. Mater.* **2006**, *5*, 665−670.
(30) Gong, X. Q.; Selloni, A. Role of Steps in the Reactivity of the Anatase TiO_2 (101) Surface. *J. Catal.* **2007**, *249*, 134−139.
(31) Zhao, Z. Y.; Li, Z. S.; Zou, Z. G. Understanding the Interaction of Water with Anatase TiO_2 (101) Surface from Density Functional Theory Calculations. *Phys. Lett. A* **2011**, *375*, 2939−2945.
(32) Kharche, N.; Hybertsen, M. S.; Muckerman, J. T. Computational Investigation of Structural and Electronic Properties of Aqueous Interfaces of GaN, ZnO, and a GaN/ZnO Alloy. *Phys. Chem. Chem. Phys.* **2014**, *16*, 12057−12066.
(33) Kristoffersen, H. H.; Shea, J. E.; Metiu, H. Catechol and HCl Adsorption on TiO_2 (110) in Vacuum and at the Water-TiO_2 Interface. *J. Phys. Chem. Lett.* **2015**, *6*, 2277−2281.
(34) Ertem, M. Z.; Kharche, N.; Batista, V. S.; Hybertsen, M. S.; Tully, J. C.; Muckerman, J. T. Photoinduced Water Oxidation at the Aqueous GaN ($10\bar{1}0$) Interface: Deprotonation Kinetics of the First Proton-Coupled Electron-Transfer Step. *ACS Catal.* **2015**, *5*, 2317−2323.
(35) Kharche, N.; Muckerman, J. T.; Hybertsen, M. S. First-Principles Approach to Calculating Energy Level Alignment at Aqueous Semiconductor Interfaces. *Phys. Rev. Lett.* **2014**, *113*, 176802.

DOI: 10.1021/acs.jpclett.8b01182
J. Phys. Chem. Lett. 2018, 9, 3131−3136

(36) Bjorneholm, E.; Hansen, M. H.; Hodgson, A.; Liu, L. M.; Limmer, D. T.; Michaelides, A.; Pedevilla, P.; Rossmeisl, J.; Shen, H.; Tocci, G.; et al. Water at Interfaces. *Chem. Rev.* **2016**, *116*, 7698−7726.
(37) Ketteler, G.; Yamamoto, S.; Bluhm, H.; Andersson, K.; Starr, D. E.; Ogletree, D. F.; Ogasawara, H.; Nilsson, A.; Salmeron, M. The Nature of Water Nucleation Sites on TiO_2 (110) Surfaces Revealed by Ambient Pressure X-Ray Photoelectron Spectroscopy. *J. Phys. Chem. C* **2007**, *111*, 8278−8282.

DOI: 10.1021/acs.jpclett.8b01182
J. Phys. Chem. Lett. 2018, 9, 3131−3136